Ge-ZSM-5: the Simultaneous Incorporation of Ge and Al into ZSM-5 Using a Parallel Synthesis Approach

Leon G. A. van de Water,[†] Jan C. van der Waal,[†,‡] Jacobus C. Jansen,[†] Marcella Cadoni,[§] Leonardo Marchese,[§] and Thomas Maschmeyer*[,†]

Laboratory of Applied Organic and Catalytic Chemistry, Delft University of Technology, Julianalaan 136, 2628 BL Delft, The Netherlands, Avantium Technologies B.V., Zekeringstraat 29, 1014 BV, P.O. Box 2915, 1000 CX, Amsterdam, The Netherlands, and Universita Piemonte Orientale Amedeo Avogadro, Dipartimento Sci & Tecnol Avanzate, C So Borsalino 54, I-15100 Alessandria, Italy

Received: April 16, 2003; In Final Form: July 9, 2003

A series of Ge-ZSM-5 zeolites has been synthesized as the first part of a study on the effect of Ge incorporation on catalytically relevant properties of ZSM-5, such as framework acidity, framework structure, and crystal morphology. Products have been characterized by XRD, SEM, NMR, nitrogen adsorption, NH_3-TPD, and infrared (FT-IR) spectroscopy. The simultaneous incorporation of Al and Ge has been proven by elemental analysis, ^{27}Al MAS NMR, FT-IR, and XRD. Ge incorporation changes the crystallization behavior in such a way that, in a controlled and reproducible manner, spherical aggregates of Ge-ZSM-5 crystallites could be prepared. Nitrogen physisorption measurements reveal that Ge-ZSM-5 contains more meso- and macroporosity than ZSM-5, which may be related to the high number of interfaces between the small crystallite particles of which these spherical aggregates are built up. Furthermore, Ge incorporation leads to a change in unit-cell symmetry of the zeolites (NH_4^+ form) from monoclinic to orthorhombic. NH_3-TPD suggests that Ge incorporation does not lead to a different framework acidity. FT-IR experiments on H-ZSM-5 and H-Ge-ZSM-5, in contact with chemisorbed CO molecules, indicate that the strength of the strong Brønsted acid sites does not change upon Ge incorporation, as a similar frequency shift in the hydroxyl stretch vibration region has been observed upon interaction with CO. Upon Ge incorporation, a broadening of double five-ring lattice vibrations at around 550 cm^{-1} is observed. Lattice local modes at around 950 cm^{-1}, due to asymmetric stretching vibrations of Si−O−Ge groups, are found when Ge is incorporated into the MFI framework. The incorporation of Ge in the MFI framework causes an increased number of local distortions and defects leading to a greater variety of hydroxyl groups and significant changes in crystal morphology. The former can be concluded from an increase of the infrared absorption band related to Si−OH groups (3746 cm^{-1}) and the latter from SEM images and nitrogen physisorption isotherms.

1. Introduction

Zeolite ZSM-5[1] (MFI framework type) is characterized by the presence of two intersecting channel systems, its largest rings containing 10 T-atoms. The substitution of Si in the MFI framework by other trivalent elements than Al, such as B,[2] Fe,[3] or Ga,[4] has been reported. The resulting materials generally possess lower framework acidity than Al-ZSM-5. The Si atoms in silicalite-1, the all-silica analogue of ZSM-5, can also be isomorphously substituted by other tetravalent elements, such as Ge[5−8] and Ti.[9] These substitutions do not generate Brønsted acidity in the framework as both elements are also tetravalent, but both the adsorption and catalytic properties of the resulting materials have been reported to change. For example, the separation selectivity of *n*-C_4H_{10}/*i*-C_4H_{10} mixtures by Ge-silicalite-1 membranes appeared to be higher than for the all-silica analogue.[8] Small changes in pore sizes and changes in adsorption properties are thought to be responsible for this, as the observed trend is not a function of the framework acidity. Ge-silicalite-1 membranes on a α-Al_2O_3 support have been reported in which part of the support appeared to dissolve upon membrane formation, resulting in the incorporation of some of the Al into the membrane (Si/Al ratio of around 100).[10]

The present work deals with the *simultaneous* incorporation of Al and Ge into the MFI framework. Ge does not, in principle, generate additional acid sites in ZSM-5 (other than Ge−OH because of possible defects), but the acidic strength of the T−O(H)-Al sites (T = Si or Ge) may be altered when Ge atoms are present in framework positions close to Al atoms. A modified framework acidity may be of interest for certain catalytic applications, for example, ZSM-5 or other zeolites with a weaker acidity would be applicable for reactions where catalyst deactivation through coking on very acidic sites occurs. On the other hand, zeolites with an increased acidity may find application in processes where current catalysts show only very low activities or require very high temperatures. Furthermore, structural distortions (e.g., strain induced by unit-cell expansion) may be introduced in the framework because of the presence of Ge, which may change the physical properties of the zeolite and, hence, also the catalytic properties. An example of the effect that the incorporation of Ge can have on the catalytic properties of an existing catalyst has been reported for TS-1: the catalytic

* To whom correspondence should be addressed. E-mail: Th.Maschmeyer@tnw.tudelft.nl.
[†] Delft University of Technology.
[‡] Avantium Technologies B.V.
[§] Universita Piemonte Orientale Amedeo Avogadro.

10.1021/jp0304531 CCC: $25.00
Published on Web 08/30/2003

TABLE 1: Comparison of the Different Synthetic Methods toward Ge-ZSM-5

	series A	series B	series C
Ge source	GeO_2	Na metagermanate	$GeCl_4$
Al source	Al_2O_3	$NaAlO_2$	$NaAlO_2$
template source	TPAOH	TPABr	TPABr
crystallinity	decreased at high Ge content	decreased at high Ge content	high
additional phases	GeO_2	GeO_2	no
Ge incorporation	partly	yes	yes
Al incorporation	no	yes	yes

activity of Ge-TS-1 in the epoxidation of propene is significantly higher than that of the parent material TS-1.[11,12] Additionally, the presence of Ge may modify the crystallization behavior because of its ability to have a higher coordination number than four prior to incorporation and because of the different condensation kinetics of Ge−OH groups as compared to Si−OH groups.

In this paper, the synthesis of a series of Ge-ZSM-5 zeolites is described, whereby a parallel synthesis approach was adopted in order to find the best synthetic method for the simultaneous incorporation of Ge and Al. We have previously used such a high-speed experimentation (HSE) approach for the synthesis of zeolite beta with low Si/Al ratios.[13] This approach appeared to be very useful to screen multiple reaction parameters, such as the nature and the ratios of the synthesis gel components, in a relatively short time. In the case of Ge-ZSM-5, factors such as the Ge concentration in the reaction mixture, the presence and concentration of Al, the pH, the amount of water, and the nature of the Ge, Si, and Al sources have been investigated in order to find the optimum procedure for the simultaneous incorporation of Ge and Al into ZSM-5.

2. Experimental Section

Synthesis. The parallel syntheses were carried out in several 6×4 matrix blocks of small 3 mL Teflon-lined stainless steel autoclaves.[13] The experiments were performed under hydrothermal conditions at 170 °C under autogenous pressure with a reaction time of 4 days. The parameters that were varied in these experiments (series A, B, and C, see Table 1) were the Ge source (GeO_2, sodium metagermanate,[14] $GeCl_4$), the Al source (Al_2O_3, $NaAlO_2$), the template species [tetrapropylammonium hydroxide (TPAOH), tetrapropylammonium bromide (TPABr)], the Ge/(Ge + Si) ratio (0, 0.05, 0.10, 0.15, 0.20, and 0.25), and the (Ge + Si)/Al ratio (29.5, 34.5, 45, and ∞). LUDOX HS 40 (a highly reactive 40 wt % dispersion of SiO_2 in water, stabilized with 0.5 wt % of Na_2O) was used as the silicon source in all cases. In the first set of experiments (series A), gels with the following composition were prepared: x GeO_2:y SiO_2:z Al_2O_3:33 TPAOH, where $x = 0$, 5, 10, 15, 20, and 25; $y = 100$, 95, 90, 85, 80, and 75; and $z = 1.69$, 1.45, 1.11, and 0, respectively. The second set of experiments (series B) involved reaction mixtures of the following compositions: x GeO_2:y SiO_2:z $NaAlO_2$:25 TPABr:50 HF:400 CH_3NH_2, where $x = 0$, 5, 10, 15, 20, and 25; $y = 100$, 95, 90, 85, 80, and 75; and $z = 3.40$, 2.90, 2.22, and 0, respectively. The Ge source was sodium metagermanate, prepared prior to synthesis by heating stoichiometric amounts of Na_2CO_3 and GeO_2 at 800 °C for 24 h. The third set of experiments, series C, was based on a procedure first published by Gabelica and Guth,[5] the difference being that no Al was present in their case. The composition of the gels was x $GeCl_4$:y SiO_2:z $NaAlO_2$:25 TPABr:50 HF:400 CH_3NH_2, where $x = 0$, 5, 10, 15, 20, and 25; $y = 100$, 95, 90, 85, 80, and 75; and $z = 3.40$, 2.90, 2.22, and 0, respectively. After reaction, the reactor blocks were cooled to room temperature and the products were washed with water and subsequently centrifuged (three times). After drying of the samples overnight at 100 °C, the template was removed by calcination in air at 550 °C for 10 h. Several of the above-mentioned syntheses were repeated on a larger scale in conventional Teflon-lined stainless steel autoclaves (typical reactor volume: 40 mL) (series D). The components were thoroughly mixed prior to heating, where the Si and Ge sources were the last two components to be added to the mixtures. The NH_4^+ form of the products was obtained after ion exchange with NH_4NO_3 solutions (0.1 M) three times. The H^+ form was obtained by calcination of the NH_4^+ zeolites in air at 550 °C for 10 h.

Analytical Techniques. Si, Ge, and Al contents were determined by ICP-OES using a Perkin-Elmer Optima 3000DV apparatus. Scanning electron micrographs were obtained on a Philips XL20 microscope. Nitrogen adsorption and desorption isotherms were measured at 77 K on a Quantachrome Autosorb-6B. Powder diffraction data were collected on a Philips PW 1840 diffractometer, generating Cu Kα radiation and on a Bruker AXS D5005 diffractometer with a Braun position sensitive detector (PSD) in scanning mode, equipped with a Huber incident beam monochromator for Cu Kα1 wavelength ($\lambda = 0.15406$ nm). Solid state ^{27}Al and ^{29}Si NMR spectra were recorded on a 400 MHz Varian Inova spectrometer. Ammonia desorption experiments (NH_3-TPD) were performed on a Micromeritics TPD/TPR 2900 apparatus. Thermal treatments under vacuum and gas dosage were made in a suitable IR cell allowing both in situ high-temperature and low-temperature treatments. Infrared spectra of adsorbed CO on template-free pelletized sample were recorded at 77 K on a Bruker Equinox 55 spectrometer at a resolution of 4 cm^{-1}.

3. Results

Synthesis. The comparison of the synthetic methods (series A, B, and C) is summarized in Table 1. The characteristic XRD diffraction pattern of ZSM-5 was obtained in all cases, albeit that the crystallinity of the products in series A and B decreases somewhat upon increasing Ge content. Furthermore, additional peaks at $2\theta = 11.55$ and 28.55 are observed in the diffraction patterns of the series B samples (in most cases) and series A samples (in some cases) at high Ge levels. These peaks point to the presence of an additional germanium oxide phase. The diffraction patterns of the series C samples show the highest crystallinity, as determined by the signal-to-noise ratios relative to that of the corresponding Ge-free ZSM-5 sample, and no additional phases are observed in the diffractograms. Furthermore, the crystallinity does not decrease as a function of Ge concentration.

Elemental analysis of some of the series A samples reveals that no Al, and only part of the Ge, is incorporated in the samples. In the case of series B, both the Al and Ge contents correspond well with the gel composition. Elemental analysis of representative samples from series C reveals that both Al and Ge are incorporated, with an efficiency of 60−70% (Al) and 75−85% (Ge), respectively.

TABLE 2: Molar Gel Compositions for the Synthesis of Series D[a]

Ge/(Ge + Si)	$GeCl_4$	SiO_2	$NaAlO_2$	TPABr	CH_3NH_2	HF
0	0	49.3	1.67	12.3	197	24.7
0.05	2.47	46.9	1.67	12.3	197	24.7
0.10	4.93	44.4	1.67	12.3	197	24.7
0.15	7.40	41.9	1.67	12.3	197	24.7
0.20	9.87	39.5	1.67	12.3	197	24.7
0.25	12.3	37.0	1.67	12.3	197	24.7

[a] All values are in mmol.

TABLE 3: Yields of Ge-ZSM-5 (Series D) before and after Calcination (Based on the Total Masses of the Starting Oxides, Plus TPA or Na, Respectively)

Ge/(Ge+Si) (gel)	yield before calcination (TPA-Ge-ZSM-5)		yield after calcination (Na-Ge-ZSM-5)	
	g	%	*g*	%
0	3.46	102.6[a]	3.01	97.06
0.05	3.27	93.87	2.94	91.57
0.10	3.36	93.51	3.06	92.15
0.15	3.46	93.44	3.13	91.24
0.20	3.81	99.93	3.42	96.61
0.25	3.85	98.15	3.47	95.07

[a] Sample was not completely free of excess organic template.

On the basis of the XRD and elemental analysis results, the synthetic procedure used for series C has been adopted to repeat some of the syntheses on a larger scale (series D). A series of six compositions, all with a (Ge + Si)/Al ratio of 29.5, has been selected for the large-scale syntheses, where the Ge/(Ge + Si) ratio has been varied throughout the series. The molar compositions of the six synthesis gels of series D are given in Table 2. The yields before and after calcination are presented in Table 3. The yields are very high in all cases (>90%), indicating that hardly any product was lost upon isolation and purification. The results of the chemical analysis of the products are given in Table 4. The Ge and Al contents of the products are in all cases lower than might be expected from the gel compositions: instead of (Ge + Si)/Al ratios of 29.5 (gel composition), values in the range from 41 to 53 are observed in the products, with a slightly higher Al incorporation at higher Ge contents (see Figure 1). The efficiency of the Ge incorporation is shown in Figure 2, and the Ge content in the products is in all cases slightly lower than in the gel. From the chemical analysis data it can be concluded that the simultaneous incorporation of Al and Ge in ZSM-5 is possible in the compositional area investigated. The presence of Ge in the synthesis mixture seems to enhance the Al incorporation to a (small) extent.

Characterization. *SEM.* Analysis of the morphology of the Ge-ZSM-5 zeolites by SEM photographs reveals remarkable differences. ZSM-5 without Ge occurs as the familiar elongated prismatic single crystals (Figure 3A). Upon increasing the Ge content, twinning of the crystals increases and spherical aggregates are formed. It appears that not only the way of

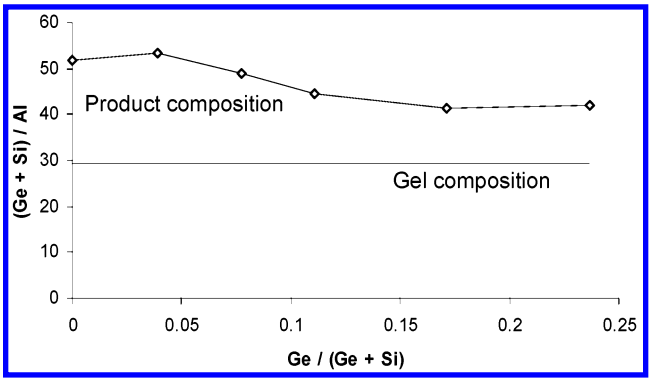

Figure 1. Al incorporation as a function of the Ge concentration in the products.

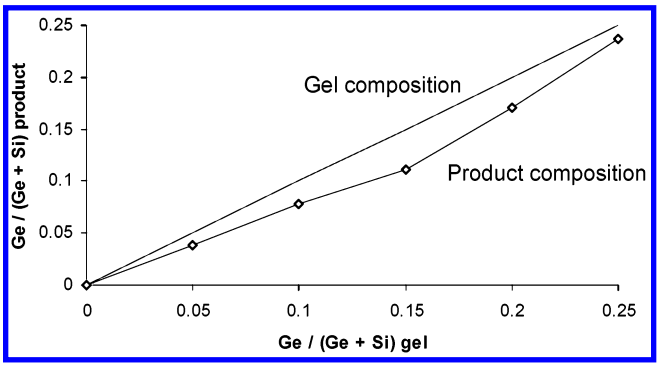

Figure 2. Ge incorporation as a function of the gel composition.

interconnection of the crystallites has changed, but also the shape of the individual crystallites. The characteristic hexagonal features are lost in the crystals depicted in Figure 3B, instead the aggregates are built up from more or less rectangular blocks. At even higher Ge levels, a spherical-aggregate form is observed (Figure 3, parts C and D). This change of crystal morphology has also been observed for Ge-silicalite-1,[7] and also for B-,[15,16] Ga-, and Fe-containing ZSM-5.[7] The introduction of T atoms with a size different from Si may cause this phenomenon. The difference between these previously observed spherically shaped MFI-type crystals and the Ge-ZSM-5 crystals from this study, is that the latter contain additional block-shaped crystallites on their surface (see Figure 3, parts C and D), in contrast to Ge-silicalite-1 and B-ZSM-5, which have smoother surfaces and smaller aggregate sizes. A possible explanation for the additional blocks on the surface may be that they have been formed on the preformed spheres during the cooling stage of the crystallization process.

Nitrogen Physisorption. Nitrogen adsorption and desorption measurements were performed in order to obtain information on the porous properties of the samples, and the results are presented in Table 5. The values for the BET surface area (S_{BET}), total volume (V_{tot}), micropore volume (V_{micro}), and mesopore surface area (S_{meso}) have been corrected for density differences due to the presence of Ge in the samples, and these normalized values are given in parentheses. The normalization factors are

TABLE 4: Chemical Composition of Series D Samples

Ge/(Ge+Si) (gel)	wt %			atomic ratios			T atoms/u.c.		
	Ge	Si	Al	Ge/(Ge + Si)	(Ge+Si)/Al	Ge/Al	Ge	Si	Al
0	0.0	45.2	0.84	0	51.69	0	0	94.2	1.8
0.05	4.41	42.1	0.79	0.039	53.27	2.07	3.7	90.6	1.8
0.10	8.47	38.9	0.83	0.078	48.82	3.79	7.3	86.8	1.9
0.15	12.0	37.2	0.90	0.111	44.66	4.96	10.4	83.5	2.1
0.20	17.5	32.8	0.92	0.171	41.32	7.07	16.0	77.7	2.3
0.25	23.1	28.8	0.86	0.237	42.16	9.98	22.2	71.6	2.2

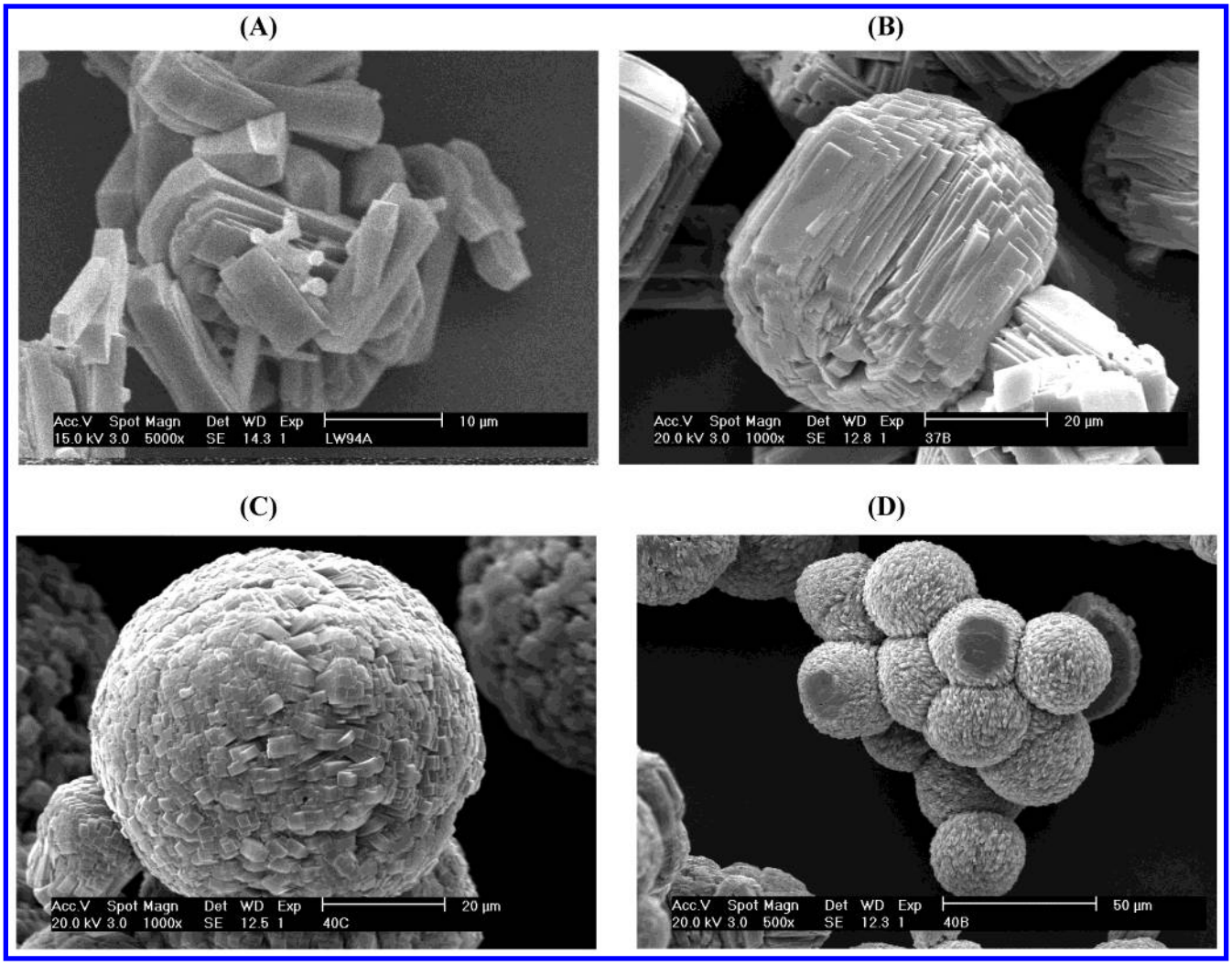

Figure 3. SEM micrographs of (Ge-)ZSM-5 with Ge/(Ge + Si) ratios of 0 (A), 0.04 (B), 0.08 (C), and 0.11 (D).

TABLE 5: N_2 Physisorption Results of Series D Samples

Ge/(Ge+Si) (gel)	S_{BET} (m^2/g)[a]		V_{tot} (cm^3/g)[a]		V_{micro} (cm^3/g)[a]		S_{meso} (m^2/g)[a]		$(S_{meso}/S_{BET})100$
0	375	(375)	0.20	(0.20)	0.15	(0.15)	6.34	(6.34)	1.7
0.05	370	(394)	0.20	(0.21)	0.14	(0.15)	19.4	(20.7)	5.3
0.10	355	(394)	0.19	(0.21)	0.14	(0.16)	19.7	(21.8)	5.5
0.15	340	(383)	0.20	(0.23)	0.12	(0.14)	30.0	(33.8)	8.8
0.20	335	(391)	0.22	(0.26)	0.12	(0.14)	41.0	(47.8)	12.2
0.25[b]	335	(378)	0.20	(0.23)	0.12	(0.14)	29.6	(33.4)	8.8

[a] Normalized values for higher mass of Ge are given in parentheses. [b] Poor Ge incorporation (from XRD analysis).

derived from the relative mass of a unit cell for each sample. The approximation thus made is that unit-cell volume differences due to Ge incorporation are ignored, but these volume differences are reported to be very small in the case of Ge-silicalite-1 [less than 1% when Ge/(Ge + Si) = 0.20].[7] After normalization, no significant differences in BET surface area and micropore volume are observed, suggesting that Ge incorporation does not influence these catalytically important features of ZSM-5. The S_{meso} values and total pore volume of the samples, however, appear to increase substantially upon increasing Ge/(Ge + Si) ratios up to 0.20 (gel composition). S_{meso} includes the mesoporous and macroporous surface area as well as the contribution of the external surface. The increased S_{meso}/S_{BET} ratio upon Ge incorporation indicates that improved mass transfer properties of Ge-ZSM-5 can be anticipated. A possible explanation for the increased mesoporous and macroporous surface area is that Ge enhances the nucleation rate, resulting in a larger number of primary crystals with smaller size inside a synthesis-gel sphere.[17] These primary crystals then aggregate immediately, resulting in an imperfect intergrowth, which causes the observed mesoporosity. In the spherically shaped crystal aggregates (see Figure 3C,D), more interfaces between the crystallites may be present per gram of material than in the elongated aggregates because of the different ways in which the crystallites are interconnected, and this larger amount of interfaces will increase the outer surface area and thus S_{meso}. The surface area and pore volume values for Ge-ZSM-5 with Ge/(Ge + Si) = 0.25 are somewhat lower than for samples with less Ge in the synthesis mixture, which is as expected because XRD analysis revealed that this sample is the least crystalline member of the series.

XRD. The crystallinity of the (Ge-)ZSM-5 samples of series D has been analyzed by XRD. The diffraction patterns of the samples with Ge/(Ge + Si) ratios of 0−0.20 (gel composition) show peaks of high signal-to-noise ratios and no amorphous or

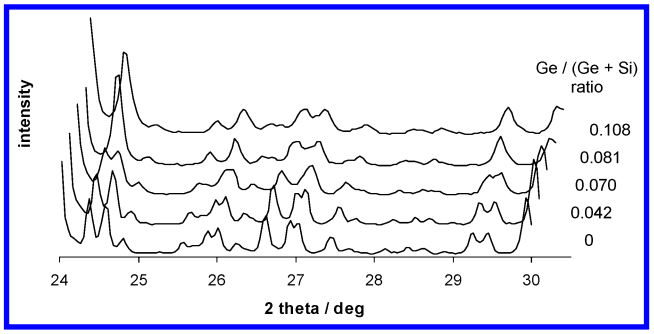

Figure 4. XRD patterns of series D (NH_4^+ form) in the 24−30° region.

crystalline byproducts. The sample with the highest Ge concentration [Ge/(Ge + Si) ratio 0.25 (gel composition)] exhibits a lower crystallinity, as the signals have lower peak areas and are broader.

Zeolites of the MFI-framework type are known to appear in two stable forms: a low-temperature phase with monoclinic symmetry and a high-temperature orthorhombic form. Factors such as nature and amount of hetero T atoms in the framework, nature of the counterions, and the presence of template molecules or other adsorbed species in the channels determine at which temperature the phase transition is observed.[18,19] The differences between the two crystallographic forms can be observed in the 2θ range from 24 to 30°, where the monoclinic form shows double peaks for certain reflections, whereas the more symmetric orthorhombic form shows single peaks.[21,21] Close inspection of the XRD patterns of Ge-ZSM-5 (NH_4^+-form) in the 2θ range 24−30° (Figure 4) shows that small changes in the peak shapes occur with increasing Ge content. The sample with Ge/(Ge + Si) = 0, depicted in Figure 4, is clearly in the monoclinic form, as the signals in the 24−25° and 29−30° regions are split.[20,21] This is still the case for Ge-ZSM-5 with Ge/(Ge + Si) = 0.042, but at a Ge/(Ge + Si) level of 0.070, an intermediate situation is observed. The diffraction patterns of the zeolites with higher Ge/(Ge + Si) levels show single peaks in these regions, indicating an orthorhombic crystal symmetry. Ge incorporation, thus, decreases the transition temperature (T_t) of ZSM-5, as (Ge-)ZSM-5 samples with no Ge or with a very low Ge concentration are below T_t at room temperature, while samples with higher Ge concentrations are above T_t. The effect of Ge incorporation on the T_t of silicalite-I has been investigated by Lopez et al.[21] The conclusion from this study is that Ge incorporation increases T_t, which is not in agreement with the observations from our study. The authors suggest that the higher degree of crystallographic defects in Ge-silicalite-I (compared to silicalite-I) hinders the zeolite framework to adopt the more symmetric orthorhombic form. The amount of defects in the Ge-ZSM-5 samples in our study also increases upon increasing Ge content, as is discussed in the FT-IR section. This would suggest the opposite: crystallographic defects facilitate (rather than hinder) the monoclinic/orthorhombic transition. The relation between crystallographic defects and the monoclinic/orthorhombic transition has also been studied by Marra et al.[22] Again, a correlation between the amount of defects and the crystal symmetry (of silicalite-I) was observed. In this case, however, the more defective samples showed orthorhombic symmetry, and monoclinic symmetry was only observed for silicalite-I when only few defects were present. The trend observed in our study is, thus, in agreement with the paper of Marra et al. and is in disagreement with the findings of Lopez et al.

It is well-known that isomorphous substitution in MFI-type zeolites results in unit-cell expansion (T = Fe,[3] Ga, Ti,[23]...) or

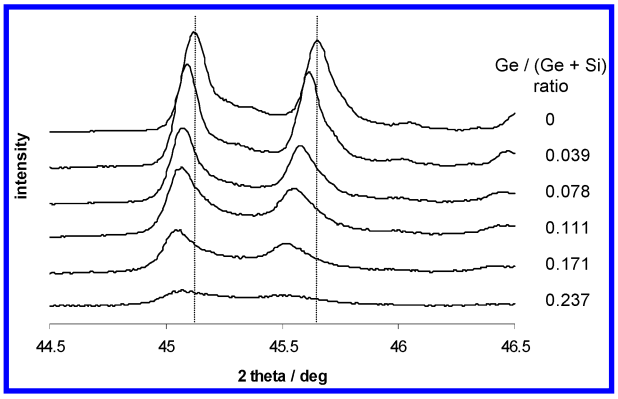

Figure 5. XRD patterns of series D (Na^+ form) in the 44.5−46.5° region.

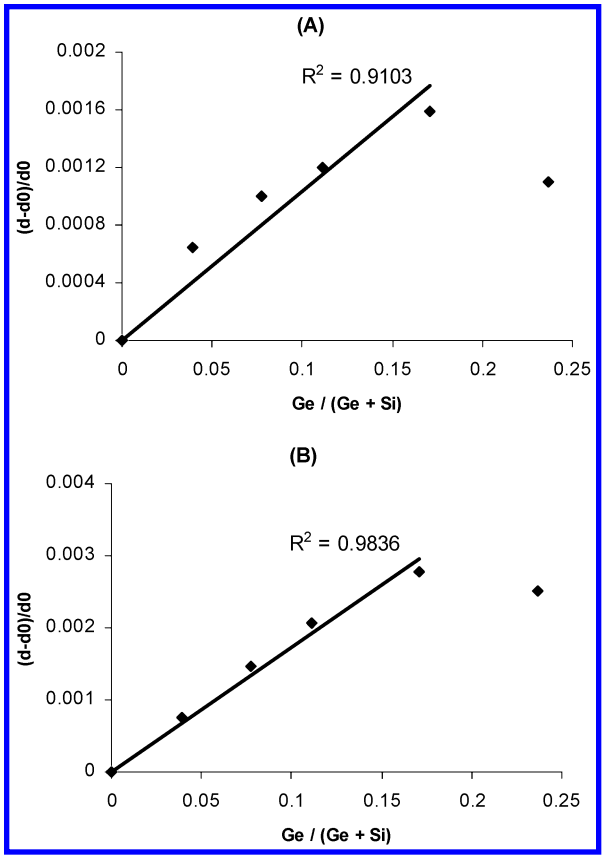

Figure 6. Correlation between the Ge content and the shift of the XRD reflections at d = 2.0107 Å (A) and d = 1.9878 Å (B) (d_0 = d value for ZSM-5 [Ge/(Ge + Si) = 0]) for series D samples (Na^+ form).

contraction (T = B[24]). Linear correlations between the number of T atoms per unit cell and the unit cell expansion/contraction have been reported for several different T atoms. The change in unit cell dimensions is also expressed in a shift of the XRD reflections. We have investigated the shifts of the reflections at d = 2.0107 Å (2θ = 45.050°) and d = 1.9878 Å (2θ = 45.599°) (corresponding to the (0 10 0) and (10 0 0) planes of the crystals in the monoclinic form, respectively[25]) as a function of the Ge content. All Ge-ZSM-5 samples must be in the Na^+ form, because in that case all members of the series are monoclinic (in contrast to the samples in NH_4^+ or H^+ form). A linear correlation between the Ge content of the samples and the shift of these reflections is found for Ge-ZSM-5 with Ge/(Ge + Si) levels of 0−0.171, see Figures 5 and 6. [R^2 of the lines equals 0.9103 (d = 2.0107 Å) and 0.9836 (d = 1.9878 Å), respectively]. The fact that Ge-ZSM-5 with Ge/(Ge + Si) = 0.237

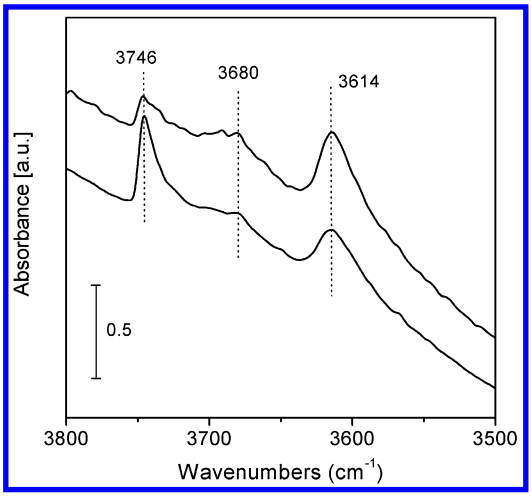

Figure 7. OH-stretching region of H-ZSM-5 (top) and H-Ge-ZSM-5 [Ge/(Ge + Si) = 0.09] (bottom).

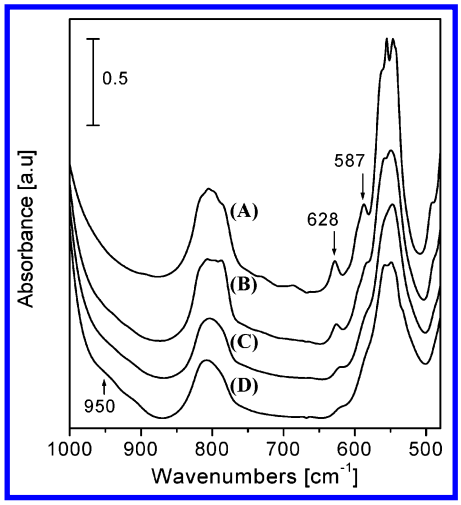

Figure 8. Infrared lattice vibration spectra of (Ge)-ZSM-5 with Ge/(Ge + Si) = 0 (A), 0.04 (B), 0.06 (C), and 0.09 (D).

falls outside this correlation indicates incomplete Ge incorporation in that case. No correlation between Ge content and XRD-peak shift is observed for the series in the NH_4^+ form, as part of the series is in monoclinic and part in orthorhombic form. The phase transition has an effect on the position of the investigated peaks and all samples need to be in the same form in order to be able to find a correlation.

NMR. The incorporation of Al in framework positions was confirmed by ^{27}Al MAS NMR. In all cases, a single peak at 55 ppm was observed, which is indicative of tetrahedrally coordinated Al. No peak corresponding to octahedral Al (around 5 ppm) could be detected. A slight broadening of the signal was observed upon increasing Ge content, indicating some structural disorder. The ^{29}Si NMR spectra of the Ge-ZSM-5 samples all show a single broad peak at −113 ppm, with some peak broadening toward lower field upon increasing Ge content. The Si atoms in Ge-ZSM-5 can have several different chemical environments, with different combinations of Al and Ge atoms as neighbors and next-nearest neighbors. This is expected to result in NMR signals with several shoulders, with each of these being due to a Si atom with a different set of neighboring atoms. A higher variation in T−O−T angles in the case of Ge-ZSM-5 may be another explanation for the observed broadening of the ^{29}Si NMR peak.[26] We have attempted to deconvolute the ^{29}Si NMR spectra, but this did not result in reliable data.

NH_3-TPD. The acidic properties of Ge-ZSM-5 have been investigated by NH_3 desorption experiments (temperature programmed desorption (NH_3-TPD)). Ammonia has been adsorbed at 373 K, and desorption has been recorded from 373 to 873 K. Very similar TPD thermograms are observed for all samples, with two main desorption bands at around 475 K and between 660 and 680 K, respectively. No correlation between desorption temperature and Ge content was observed, suggesting that acidity differences in this series of zeolites are absent or very small. However, it should be noted that the use of a strongly basic probe molecule, such as NH_3, may be unsuitable for the detection of small differences between strong Brønsted acid sites.

Infrared Spectroscopy. The IR spectra of H-ZSM-5 and H-Ge-ZSM-5 [with Ge/(Ge + Si) = 0.09] in the hydroxyl stretch-vibration region (recorded at 373 K) are depicted in Figure 7. The stretch vibration of the bridged hydroxyl group [Si−O(H)−Al] is found at around 3614 cm^{-1} for both H-ZSM-5 and H-Ge-ZSM-5. For H-Ge-ZSM-5, this band is slightly broader. The broadening of the hydroxyl signal indicates that additional acid sites are present in H-Ge-ZSM-5 compared to H-ZSM-5. The second difference in the hydroxyl region of the infrared spectra is the intensity of the band at 3746 cm^{-1} (terminal Si−OH groups), which is more intense in the case of H-Ge-ZSM-5 suggesting a higher number of crystallographic defects in this sample. The 3680 cm^{-1} band is due to hydroxyl groups with an acidity intermediate between those of bridged hydroxyls and silanol groups. This band has been reported by others[27,28] and is assigned to partially extraframework Al−OH groups, which are formed upon breaking of bridged hydroxyls. Alternatively, the 3680 cm^{-1} band in the H-Ge-ZSM-5 spectrum could indicate the presence of terminal Ge−OH groups, which have been observed in Ge-silicalite-I spectra.[6] From the H-Ge-ZSM-5 spectrum, it cannot be concluded whether the 3680 cm^{-1} band originates from Al−OH groups only or that there is also a contribution of Ge−OH groups.

The infrared spectra of H-ZSM-5 and H-Ge-ZSM-5 in the lattice-vibration region are depicted in Figure 8. The fine structure of the band around 550 cm^{-1}, which is assigned to double five rings in the MFI framework,[6] is progressively reduced by increasing the Ge concentration. The bands at 587 and 628 cm^{-1} are drastically reduced in intensity. The same changes in infrared spectra have been reported for Ge-silicalite-I and the authors suggest that the loss of fine structure results from lattice distortion caused by Ge atoms.[6] The presence of Ge atoms in framework positions induces small changes in T−O distances and T−O−T angles, thereby introducing more disorder in the structure. A band at around 950 cm^{-1} is also found in the spectra of Ge-ZSM-5 and the intensity increases with increasing Ge content. This band is assigned to local modes of the lattice originating from asymmetric Si−O−Ge vibrations in Ge-ZSM-5.[6]

The spectra of H-Ge-ZSM-5 in contact with CO molecules at different CO partial pressures at 77 K are shown in Figure 9. The frequency shift of the acidic T−O(H)−Al hydroxyl band of H-Ge-ZSM-5 (Figure 9a) is similar to that of H-ZSM-5 (not shown). The shift of this band is considered to be a measure of the H-bond donor strength,[29,30] and hence, no significant difference in acidic strength between H-ZSM-5 and H-Ge-ZSM-5 is observed. In both cases, the band at 3614 cm^{-1} disappears upon formation of OH···CO complexes and a large band at 3290−3310 cm^{-1} (the exact position depending on the partial CO pressure) is generated. The shift value of the hydroxyl band is 300−315 cm^{-1} in both cases, which is in the same range as reported by others for H-ZSM-5.[30] The bands at 3614 cm^{-1}

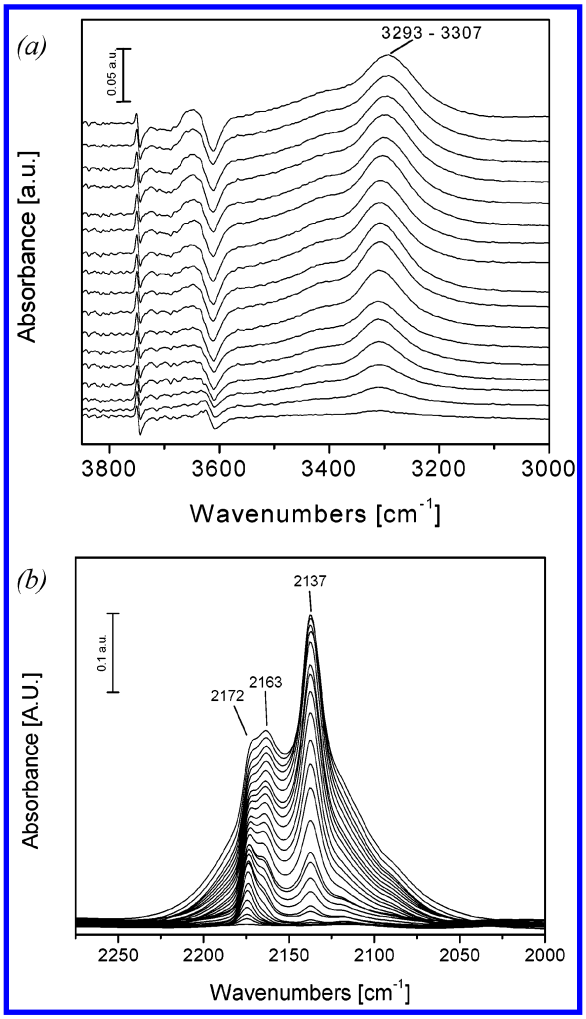

Figure 9. IR spectra of H-Ge-ZSM-5 [Ge/(Ge + Si) = 0.09] in contact with CO (different curves correspond to different CO partial pressures) in the OH stretch vibration region (a) and in the CO stretch vibration region (b).

in Figure 9a are negative peaks as a result of the subtraction of the spectrum of the bare sample from the spectra after CO adsorption. This band becomes less negative at decreasing CO doses, as the band of the bridged OH groups is recovered, in parallel with the decreasing intensity of the 3300 cm^{-1} band. Other negative bands are found at around 3745 cm^{-1} (silanols) and 3680 cm^{-1} (Al−OH), and positive absorptions are found correspondingly at 3620 cm^{-1} (Si−OH···CO) and 3500−3400 cm^{-1} (Al−OH···CO). The bands related to silanols recover first upon decreasing CO pressure, followed by those related to Al−OH and bridged OH groups. The order of acidity of the hydroxyls, inferred from both the frequency shift and the strength of the CO interaction is, as expected, Si−OH ≪ Al−OH < T−O(H)-Al.

In Figure 9b, the spectra in the CO stretch vibration region are depicted. The corresponding spectra of H-ZSM-5 (not shown) are similar to those of H-Ge-ZSM-5. A band corresponding to physically adsorbed CO molecules is observed at 2137 cm^{-1}. The band at 2172−2175 cm^{-1} is assigned to CO molecules bound to bridged hydroxyls and is in perfect agreement with other studies.[28−30] Again, no difference between H-ZSM-5 and H-Ge-ZSM-5 is observed. An additional band is visible between the 2137 and 2172 cm^{-1} bands, at 2163 cm^{-1}. This band is related to CO stretching in Al−OH···CO species,[28] which has been assigned to partially extraframework Al−OH groups absorbing at 3680 cm^{-1} in the unperturbed spectra. However, it cannot be ruled out that the 2163 cm^{-1} band in the spectrum of H-Ge-ZSM-5 is partly due to CO vibrations in Ge−OH···CO complexes, as the hydroxyls absorbing at 3680 cm^{-1} in the unperturbed spectra of H-Ge-ZSM-5 could also have a contribution of germanol groups. Upon decreasing the CO partial pressure, absorption bands related to physisorbed CO molecules disappear first, followed by the 2163 cm^{-1} band, illustrating the relative weakness of these interactions. At even lower CO pressure, the 2172−2175 cm^{-1} band is the only remaining interaction of CO molecules with the zeolite samples, which is in line with the high acidic strength of bridged hydroxyl groups compared to partially extraframework Al−OH groups.

4. Discussion

Ge incorporation does apparently not change the acidity of ZSM-5, although Ge is known to have an effect on the electron density of the oxygen atoms in zeolites. For example, the substitution of Si by Ge in Ti zeolites has been reported to increase the ionicity of the system, i.e., to increase the negative charge on the oxygen atoms.[31] The possible electronic effect of Ge on the acidity of the T−O(H)−Al proton depends on the chance that a Ge atom is found in neighboring (or next-nearest neighboring) T-atom positions relative to Al. The unit-cell composition of Ge-ZSM-5 [Ge/(Ge + Si) = 0.17] is Ge:Si:Al = 16.0:77.7:2.3, see Table 3. This means that, of the 4 T atoms next to Al, statistically 0.68 are Ge and 3.32 are Si. For the 12 next nearest neighbors, 2.0 are Ge, 9.72 are Si, and 0.28 are Al. Thus, when the assumption is made that Si and Ge atoms are randomly distributed over the framework, the different electronic properties of Ge are expected to have a noticeable effect on the acidity of the T−O(H)−Al proton (i.e., making it (slightly) less acidic). The site preference of non-silicon T atoms in the MFI framework has been investigated in several (theoretical) studies,[7,32,33] which revealed that site preference depends on the charge (3+ or 4+) and the size of the substituting atom. However, there is no agreement on preferred lattice positions for Ge between the two studies dealing with Ge substitution,[7,32] making it very difficult to draw conclusions from this. A further complicating factor is that Ge and Al are simultaneously present in the framework of Ge-ZSM-5.

Both the Ge−O (1.77 Å) and Al−O (1.74 Å) bond lengths are substantially longer than the Si−O bond length in zeolites (1.60 Å). From a geometrical point of view, it can therefore be anticipated that Al−O(H)−Ge linkages would strongly destabilize the crystal lattice (which mainly consists of Si−O bonds). This would mean that Al−O(H)−Ge linkages are not very likely to be present in Ge-ZSM-5 and that the electronic influence of Ge on the Brønsted acid sites is only small. The effect of Ge on the zeolite framework acidity is subject of further investigations.[34]

5. Conclusion

The simultaneous incorporation of Al and Ge in the MFI structure has been reported in this study. In the stage of the screening of reaction parameters, utilization of parallel synthesis equipment proved to be advantageous in terms of reducing the required amount of starting materials and time. The amount of Ge that could be incorporated in ZSM-5 was 16 Ge/unit cell in the presence of 2.3 Al/unit cell. The incorporation of Ge into the MFI framework was confirmed by small changes in the lattice vibration region in the FT-IR spectra, where the structure of the band around 550 cm^{-1} changed and a new band at 950 cm^{-1} emerged. Some properties of ZSM-5 appear to change upon Ge incorporation: the crystal symmetry changes from

monoclinic to orthorhombic, the unit cell expands, the amount of meso- and macropores and the external surface area increases with increasing Ge content, and the crystallization behavior changes, leading to the formation of spherical zeolite aggregates. NH_3-TPD and infrared analysis suggest that there is, if at all, only a very small effect of Ge on the framework Brønsted acidity. The hydroxyl stretch vibration band in the H-Ge-ZSM-5 spectrum is broader than that of H-ZSM-5, which is a result of the larger number of slightly different acid sites in H-Ge-ZSM-5. In the infrared spectra of the zeolites in the presence of adsorbed CO molecules, similar hydroxyl frequency shifts are observed for H-ZSM-5 and H-Ge-ZSM-5, indicating that the T−O(H)−Al (T = Si, Ge) Brønsted acid sites are of similar strength.

The effect of Ge incorporation on the catalytic activity of ZSM-5 in a range of test reactions is reported elsewhere.[35] The different diffusional (changes of micropore shape and dimensions and the degree of meso- and macroporosity) and acidic properties of H-Ge-ZSM-5 results in materials with improved catalytic properties in certain processes.

Acknowledgment. L.v.d.W. thanks Avantium Technologies B.V. for a Fellowship. The analytical support of Dr. A. Sinnema, Mr. J. Groen, and Mr. N. van der Pers for NMR, gas adsorption, and XRD measurements, respectively, is gratefully acknowledged.

References and Notes

(1) Argauer, R. J.; Landolt, G. R. U.S. Patent 3,702,886, 1972.
(2) de Ruiter, R.; Jansen, J. C.; van Bekkum, H. *Zeolites* **1992**, *12*, 56.
(3) Szostak, R.; Nair, V.; Thomas, T. L. *J. Chem. Soc., Faraday Trans. 1* **1987**, *83*, 487−494.
(4) Simmons, D. K.; Szostak, R.; Agrawal, P. K.; Thomas, T. L. *J. Catal.* **1987**, *106*, 287.
(5) Gabelica, Z.; Guth, J.-L. *Angew. Chem., Int. Ed. Eng.* **1989**, *28* (1), 81−83.
(6) Kosslick, H.; Tuan, V.; Fricke, R.; Peuker, Ch. *Ber. Bunsen-Ges. Phys. Chem.* **1992**, *96*, 1761−1765.
(7) Kosslick, H.; Tuan, V. A.; Fricke, R.; Peuker, Ch.; Pilz, W.; Storek, W. *J. Phys. Chem.* **1993**, *97*, 5678−5684.
(8) Tuan, V. A.; Falconer, J. L.; Noble, R. D. *Microp. Mesop. Mater.* **2000**, *41*, 269−280.
(9) Taramasso, M.; Perego, G.; Notari, B. U.S. Patent No. 4,410,501, 1983.
(10) Li, S.; Tuan, V. A.; Falconer, J. L.; Noble, R. D. *Microp. Mesop. Mater.* **2003**, *58*, 137−154.
(11) Mantegazza, M. A.; Petrini, G.; Spano, G.; Bagatin, R.; Rivetti, F. *J. Mol. Catal. A-Chem.* **1999**, *146* (1−2), 223−228.
(12) Faraj, M. K. U.S. Patent No. 5,977,009, 1999.
(13) Pescarmona, P. P.; Rops, J. J. T.; van der Waal, J. C.; Jansen, J. C.; Maschmeyer, T. *J. Mol. Catal. A-Chem.* **2002**, *182−183*, 319−325.
(14) Johnson, G. M.; Tripathi, A.; Parise, J. B. *Chem. Mater.* **1999**, *11*, 10−12.
(15) Sundaramurthy, V.; Lingappan, N. *J. Mol. Catal. A-Chem.* **2000**, *160*, 367−375.
(16) Shibata, M.; Gabelica, Z. *Appl. Catal. A: General* **1997**, *162*, 93−102.
(17) Koegler, J. H.; van Bekkum, H.; Jansen, J. C. *Zeolites* **1997**, *19*, 262−269.
(18) Wu, E. L.; Lawton, S. L.; Olson, D. H.; Rohrman, A. C., Jr.; Kokotailo, G. T. *J. Phys. Chem.* **1979**, *83* (21), 2777−2781.
(19) Marra, G. L.; Artioli, G.; Fitch, A. N.; Milanesio, M.; Lamberti, C. *Microp. Mesop. Mater.* **2000**, *40*, 85−94.
(20) Hay, D. G.; Jaeger, H. *J. Chem. Soc. Chem. Commun.* **1984**, 1433.
(21) Lopez, A.; Soulard, M.; Guth, J. L. *Zeolites* **1990**, 134−136.
(22) Marra, G. L.; Tozzola, G.; Leofanti, G.; Padovan, M.; Petrini, G.; Genoni, F.; Venturelli, B.; Zecchina, A.; Bordiga, S.; Ricchiardi, G. *Stud. Surf. Sci. Catal.* **1994**, *84*, 559−566.
(23) Fricke, R.; Kosslick, H.; Tuan, V. A.; Grohmann, I.; Pilz, W.; Storek, W.; Walther, G. *Stud. Surf. Sci. Catal.* **1994**, *83*, 57−66.
(24) Jansen, J. C.; Biron, E.; van Bekkum, H. in *Innovation in Zeolite Materials Science*; Grobet, P. J., et al., Eds.; Elsevier: Amsterdam, 1988; pp 133−141.
(25) International Database of Zeolite Structures http://www.iza-structure.org/databases/.
(26) Thomas, J. M.; Klinowski, J.; Ramdas, S.; Hunter, B. K.; Tennakoon, D. T. B. *Chem. Phys. Lett.* **1983**, *102*, 158−162.
(27) Zecchina, A.; Bordiga, S.; Spoto, G.; Scarano, D.; Petrini, G.; Leofanti, G.; Padovan, M.; Otero Areán, C. *J. Chem. Soc., Faraday Trans.* **1992**, *88* (19), 2959−2969.
(28) Onida, B.; Borello, L.; Bonelli, B.; Geobaldo, F.; Garrone, E. *J. Catal.* **2003**, in press.
(29) Mirosjew, I.; Ernst, S.; Weitkamp, J.; Knözinger, H. *Catal. Lett.* **1994**, *24*, 235−248.
(30) Knözinger, H.; Huber, S. *J. Chem. Soc., Faraday Trans.* **1998**, *15*, 2047−2059.
(31) Zicovich-Wilson, C. M.; Corma, A. *J. Phys. Chem. B* **2000**, *104*, 4134−4140.
(32) Smirnov, K. S.; Kudryashova, M. V. *Microp. Mater.* **1995**, *5*, 9−15.
(33) de Vos Burchart, E.; van Bekkum, H.; van de Graaf, B. *Collect. Czech. Chem. Commun.* **1992**, *57*, 681.
(34) van de Water, L. G. A.; Zwijnenburg, M. A.; van der Waal, J. C.; Sloof, W. G.; Cadoni, M.; Marchese, L.; Jansen, J. C.; Maschmeyer, T. manuscript in preparation.
(35) van de Water, L. G. A.; van der Waal, J. C.; Jansen, J. C.; Maschmeyer, T. *J. Catal.* submitted.